

## Electronic Supplementary Information

### Mechanochemical hydroquinone regeneration promotes gold salt reduction in sub-stoichiometric conditions of the reducing agent

Ismael P. L. Xavier,<sup>a</sup> Laura L. Lemos,<sup>a</sup> Eduardo C. de Melo,<sup>a</sup> Eduardo T. Campos,<sup>a</sup> Breno L. de Souza,<sup>a</sup> Leandro A. Faustino,<sup>a</sup> Douglas Galante,<sup>b</sup> Paulo F. M. de Oliveira<sup>a\*</sup>

<sup>a</sup>*Institute of Chemistry, University of São Paulo – Av. Prof. Lineu Prestes 748, 05360-050, São Paulo – SP, Brasil.*

<sup>b</sup>*Brazilian Synchrotron Light Laboratory (LNLS), Brazilian Center for Research in Energy and Materials (CNPEM), Campinas – SP, 13083-970, Brazil.*

e-mail: [paulofmo@usp.br](mailto:paulofmo@usp.br)

## S1. Electrochemical Equations

**Table S1.** Reduction reactions of H<sub>2</sub>AuCl<sub>4</sub> and oxidation reactions of reducing agents (R<sub>A</sub>) with corresponding standard electrochemical potentials.

Half-Reaction	E <sup>0</sup> (V vs. SHE)*	
$AuCl_4 + 3e^- \rightarrow Au^0 + 4Cl^-$	E <sup>0</sup> <sub>red</sub> = +0.850 V	(Eq.S1)
Sodium Borohydride** - NaBH <sub>4</sub>		
$BH_4^- + 3H_2O \rightarrow B(OH)_3 + 7H^+ + 8e^-$	E <sup>0</sup> <sub>oxi</sub> = +0.481 V	(Eq.S2)
Ascorbic Acid - C <sub>6</sub> H <sub>8</sub> O <sub>6</sub>		
$C_6H_8O_6 \rightarrow C_6H_6O_6 + 2H^+ + 2e^-$	E <sup>0</sup> <sub>oxi</sub> = -0.077 V	(Eq.S3)
Hydroquinone - C <sub>6</sub> H <sub>4</sub> (OH) <sub>2</sub>		
$C_6H_4(OH)_2 \rightarrow C_6H_4O_2 + 2H^+ + 2e^-$	E <sup>0</sup> <sub>oxi</sub> = -0.699 V	(Eq.S4)

\*Potentials based on the Standard Hydrogen Electrode

\*\*In neutral medium

With the E<sup>0</sup> provided in Table S1, it is possible to calculate the variation of cell potential (ΔE<sup>0</sup><sub>cell</sub>, V) for each overall balanced electrochemical reaction (Eq. S6). Then,

the variation of Gibb's energy ( $\Delta G$ ,  $kJ.mol^{-1}$ ) is easily obtained by the Eq. S7, where  $n$  is the number of transferred electrons and  $F$  is the Faraday's constant ( $96,485 C.mol^{-1}$ ).

$$\Delta E^0_{cell} = E^0_{red} + E^0_{oxi} \quad (\text{Eq. S6})$$

$$\Delta G = -nF\Delta E \quad (\text{Eq. S7})$$

**Table S2.** Overall balanced electrochemical reactions for HAuCl<sub>4</sub> reduction with different reducing agents (R<sub>A</sub>): Hydroquinone (HQ), NaBH<sub>4</sub> and L-ascorbic acid (AA) with the corresponding cell potential ( $\Delta E^0_{cell}$ ), number of transferred electrons ( $n$ ) for each reaction and respective Gibbs energy.

R <sub>A</sub>	Overall balanced reactions	$\Delta E^0_{cell}$ (V)	$n$	$\Delta G^0$ ( $kJ.mol^{-1}$ )
NaBH <sub>4</sub>	$8HAuCl_4 + 3NaBH_4 + 9H_2O \rightarrow 8Au^0 + 3B(OH)_3 + 29HCl + 3NaCl$ (Eq.S8)	+1.331	8	-1,027.4
AA	$2HAuCl_4 + 3C_6H_8O_6 \rightarrow 2Au^0 + 3C_6H_6O_6 + 8HCl$ (Eq.S9)	+ 0.773 V	6	-447.5
HQ	$2HAuCl_4 + 3C_6H_4(OH)_2 \rightarrow 2Au^0 + 3C_6H_4O_2 + 8HCl$ (Eq.S10)	+ 0.151 V	6	-87.4

**Table S3.** Overall balanced electrochemical reactions per mol of HAuCl<sub>4</sub>.

R <sub>A</sub>	Overall balanced reactions
NaBH <sub>4</sub>	$HAuCl_4 + 3/8NaBH_4 + 9/8H_2O \rightarrow Au^0 + 3/8B(OH)_3 + 29/8HCl + 3/8NaCl$ (Eq.S12)
AA	$HAuCl_4 + 3/2C_6H_8O_6 \rightarrow Au^0 + 3/2C_6H_6O_6 + 4HCl$ (Eq.S13)
HQ	$HAuCl_4 + 3/2C_6H_4(OH)_2 \rightarrow Au^0 + 3/2C_6H_4O_2 + 4HCl$ (Eq.S14)

## S2. X-ray Absorption Spectroscopy – XAS/X-ray Absorption Near Edge Spectroscopy – XANES

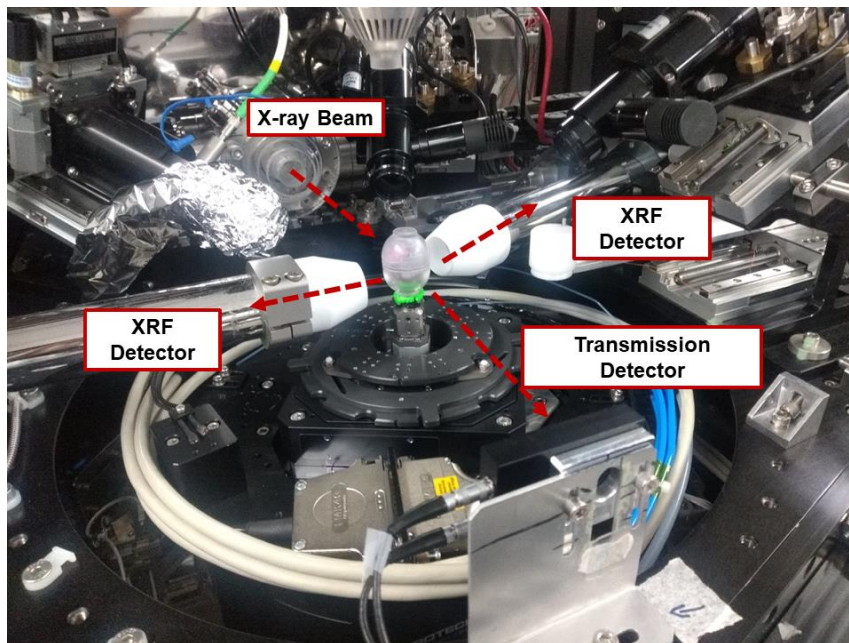


**Fig. S1.** Picture of the setup at CARNAUBA for XANES of Au-L<sub>3</sub> edge. The milling procedures were performed in the laboratory right beside the beamline. The jar was not open for the measurement. Both transmission and fluorescence modes were employed.

The selection of a PMMA jar is associated with the material's transparency to X-rays at the Au-L<sub>3</sub> absorption edge (11,919 eV) during measurements with synchrotron radiation, thereby mitigating undesired interactions. Regarding the material of the milling ball, zirconia was chosen due to its high hardness and chemical stability and, therefore, low potential for contamination of the materials under investigation. Metal-based milling systems, such as stainless steel would have reduced the gold salt and contaminated the media.

XAS in XANES region was used for monitoring the chemical state of gold. The acquisition of the XANES spectra were performed at CARNAUBA beamline line – Tarumã Endstation (Sirius, LNLS/CNPEM – Campinas, Brazil) in transmission mode (photodiode Alibava AS04-104N), probing Au L<sub>3</sub>-edge (11,919 eV). Also, 4 channels XRF detectors could be used simultaneously (Au-L<sub>α</sub> line - 9,713 eV). The beamline has

an energy resolution of  $\Delta E/E = 10^{-4} - 10^{-5}$  and uses a 4 x Si (111) crystal monochromator, and a beam size of 0.2 x 0.2  $\mu\text{m}$  was used in the measurements.

The spectra were recorded by scanning from 11,900 to 11,970 eV, using a step size of 0.5 eV and acquisition time of 1 s. Therefore, for each complete scan it took  $\sim 140$  s.

To perform the measurements the milling jar was put directly in the beam (Fig. X) to avoid additional time for sample preparation and absorption of moisture by the sample. Each spectrum displayed in the main text is a result of 2-5 consecutive scans, however, in a different region of the jar. With such a small beam size compared to the heterogeneity of powder system, we choose to rotate the sample stage  $\pm 30$ - $120^\circ$  to get a fair representation of the real state of the gold species.

XANES data were processed using ATHENA, within the IFEFFIT package (v. 1.2.11) (B. Ravel, M. Newville, J. Synchrotron Radiat. 2005, 12, 537–541). The AutoBK background subtraction procedure was used with the Rbkg parameter set to 1.0  $\text{\AA}$ . All spectra were normalized to the pre- and post-edge region consistently throughout data treatment. The calibration of the spectra was carried out with a gold metal foil. In addition, the  $\text{Au}^{\text{III}}$  standard was measured ( $\text{HAuCl}_4 \cdot 3\text{H}_2\text{O}$ ). The edge position was determined by the first derivative.

To estimate the amount of each gold specie, quantitative analysis was performed by linear combination fitting as implemented in Athena software. LCF fits of the XANES spectrum of each experimental sample, was performed by the combination of the standard samples - Au(0)- (Au(0) foil) and AuIII- ( $\text{HAuCl}_4 \cdot 3\text{H}_2\text{O}$ ). Also, a least-squares minimization is used in the analysis.

### **S3. XANES spectrum of $\text{Au}^{\text{III}}$ milled without reducing agent**

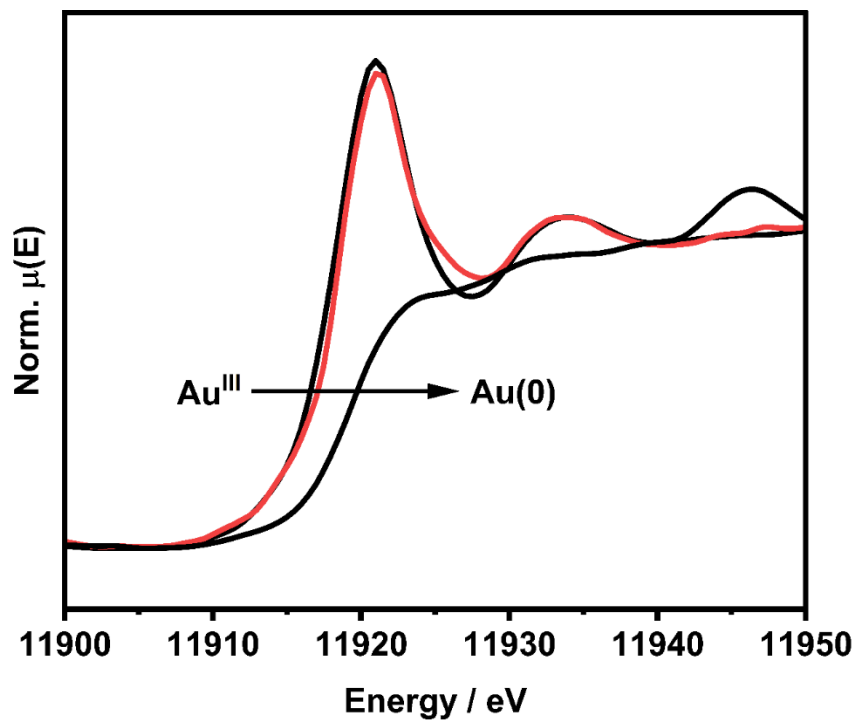


**Fig. S2-** XANES for HAuCl<sub>4</sub> milled for 60 min without the using of R<sub>A</sub> in SiO<sub>2</sub> matrix. The black spectra correspond to Au<sup>III</sup> and Au(0) standards.

#### **S4. PXRD of AuNPs synthesized with BQ**

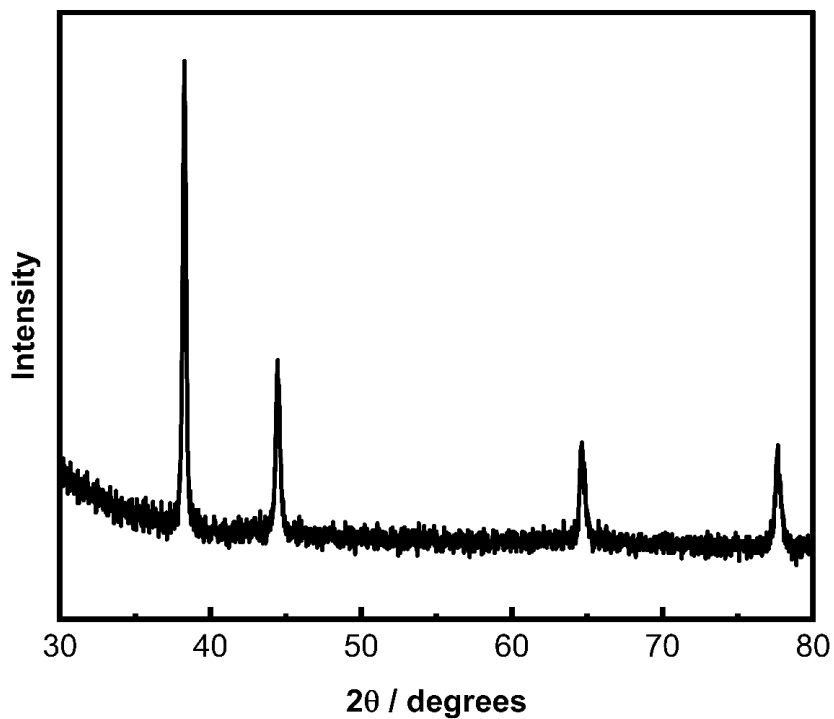


**Fig. S3-** PXRD pattern obtained from BUMS of AuNPs from AuCl<sub>4</sub><sup>-</sup> precursor and BQ as source of HQ and related reductants.

## S4. $^1\text{H}$ NMR and GC-FID/MS

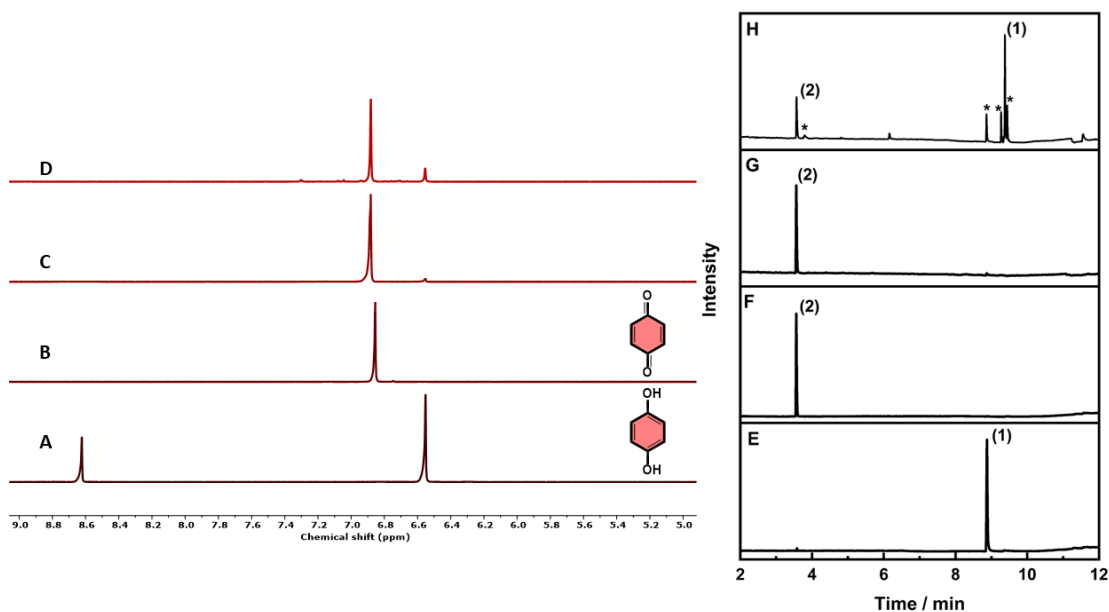


**Fig. S4-**  $^1\text{H}$  NMR spectrum of hydroquinone standard (A), benzoquinone (B), Au NPs + benzoquinone reaction without and with HCl (C and D). Chromatograms obtained in GC-FID for hydroquinone standard (E), benzoquinone (F), Extraction in ACN from Au NPs + benzoquinone reaction without (G) and with HCl (H).

Through  $^1\text{H}$  NMR analysis of Au NPs reactions with benzoquinone (the oxidation product of hydroquinone) in systems with and without HCl (Fig. S4, left side), it was observed that in the absence of acid only two peaks were detected at 6.55 ppm and 6.88 ppm. The first, less intense peak showed a chemical shift identical to the hydrogens neighboring the hydroxyl group in the hydroquinone standard (HA, 6.55 ppm), while the second, more intense peak had a chemical shift close to the hydrogens of benzoquinone (HB, 6.85 ppm). This  $^1\text{H}$  NMR signal indicating the presence of hydroquinone is possibly due to the residual presence of hydroquinone resulting from the purification process and the slow degradation of the reagent that naturally occurs over time when exposed to a non-inert atmosphere.

When the reaction was conducted in the presence of hydrochloric acid, an increase in the relative intensity of the peak at 6.55 ppm compared to the peak at 6.88 ppm was observed. This observation suggests a potential interaction between the acid in the reaction medium and benzoquinone. To investigate whether acidifying the medium alone would be adequate to drive the reaction, we performed  $^1\text{H}$  NMR analysis of benzoquinone in both neutral and acidified media. However, as revealed in the  $^1\text{H}$  NMR spectra, the acidic medium alone did not suffice to facilitate the chemical reduction of benzoquinone.

To confirm the formation of hydroquinone in the reaction medium, the acquired material at the end of the synthesis (both with and without HCl) was dispersed in acetonitrile, and the nanoparticles were precipitated by centrifugation (Table 2 - main text). The supernatant material was then injected into GC-MS and GC-FID. As observed in Fig. S4 (right), the synthesis without HCl showed only one peak in the chromatogram at 3.56 minutes (identify as peak 1), the same retention time observed in the injection of pure benzoquinone. However, in the synthesis with HCl, multiple peaks were observed in the chromatogram, corresponding to various unidentified byproducts. Of particular interest is the peak at 8.86 minutes (identify as peak 2), which corresponds to the retention time of hydroquinone and was also observed in the injection of pure hydroquinone. Fig. S5 displays a GC-MS and the fragments for the respective peaks in the chromatogram for the major compounds.

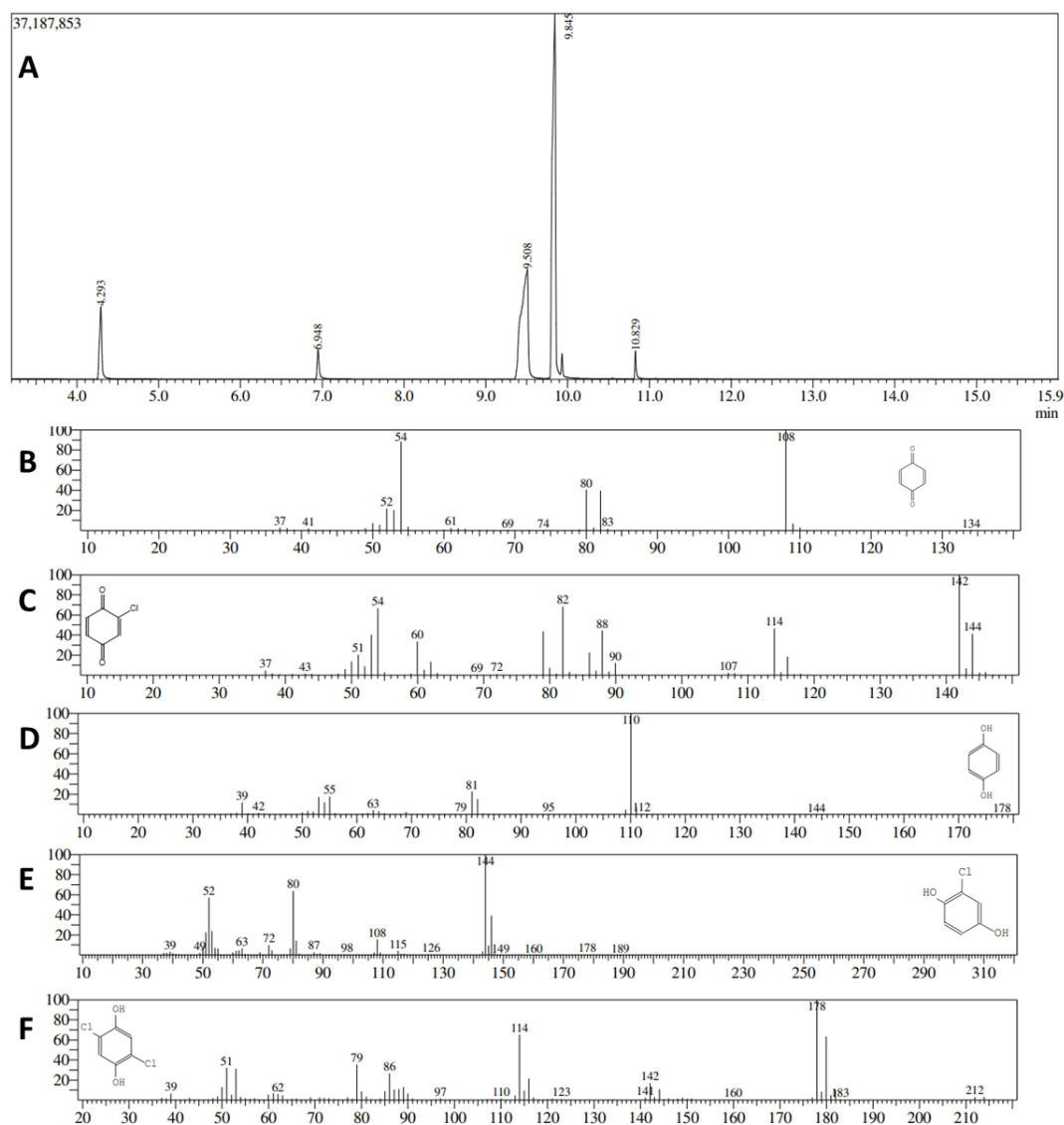


**Fig. S5-** Chromatogram (A) and peak spectra at 4.293 min, 6.948 min, 9.508 min, 9.845 min and 10.829 min of GC-MS analysis of AuNP using BQ as the source of HQ.

The GC-FID analyses were performed using the GC-2010 Plus chromatograph from Shimadzu, with an RTX-5 chromatographic column with a poly(dimethylsiloxane) stationary phase. For the GC-MS analyses the CG-msQP2010 Ultra chromatograph from Shimadzu used and a DB-5 column was employed. In both cases, the adopted procedure and the analytical method were the same. The analyzed syntheses were dispersed in 1.5 mL of high-purity acetonitrile and centrifuged to precipitate nanoparticles and silica. The supernatant material was injected into the chromatograph using N<sub>2</sub> as the carrier gas (FID) or He (MS), a detector at 250°C, and a split mode at 220°C with a 1µL injection. The run began at 60°C for 2 minutes, followed by a heating ramp of 10°C/min until



reaching 125°C, and finally, a heating ramp of 50°C/min until reaching 250°C, holding the temperature for 5 minutes.

#### S4. Transmission Electron Microscopy (TEM)

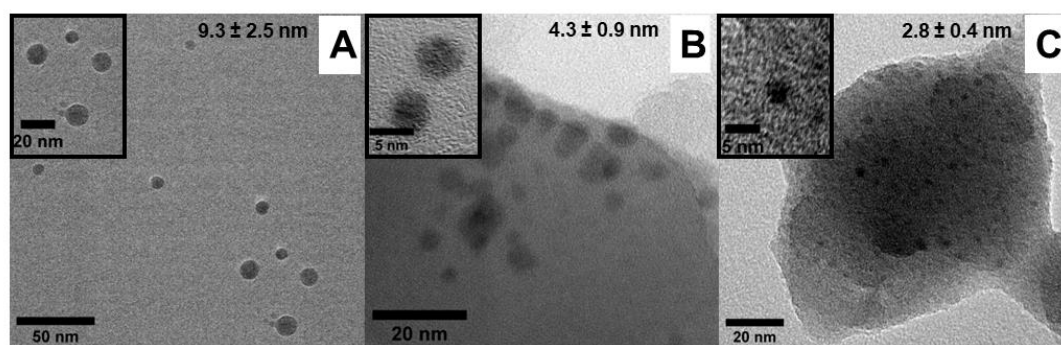


**Fig. S6-** TEM images of AuNPs supported on silica after BUMS under sub-stoichiometric - HQ<sub>sub</sub> (A), stoichiometric - HQ<sub>sto</sub> (B) and excess - HQ<sub>exc</sub> (C) of reducing agent (HQ – hydroquinone).